Application of a "Radiation-Type" Boundary Condition to the Wave, Porous Bed Problem

CHARLES R. McCLAIN[1]

Geosciences Department, North Carolina State University, Raleigh 27607

NORDEN E. HUANG

NASA Wallops Flight Center, Wallops Island, Va. 23337

LEONARD J. PIETRAFESA

Geosciences Department, North Carolina State University, Raleigh 27607

(Manuscript received 13 September 1976, in revised form 13 June 1977)

ABSTRACT

The problem of a small-amplitude wave propagating over a flat porous bed is reanalyzed subject to the bottom boundary condition

$$\left.\frac{\partial u}{\partial z}\right|_0 = \frac{\alpha}{K^{\frac{1}{2}}}(u|_0 - \tilde{u}_s|_0),$$

where u represents the horizontal velocity in the fluid, $\tilde{u}_s$ represents the horizontal velocity within the bed as predicted by Darcey's law, K is the permeability and the subscript 0 denotes evaluation at the bottom ($z=0$). The term α is a constant whose value depends on the porosity of the bed at the interface and must be determined experimentally. The boundary condition is of the form of a "radiation-type" condition commonly encountered in heat conduction problems.

The important physical quantities (velocity, velocity potential, streamfunction, shear stress and energy dissipation) have been derived and are presented, subject to natural conditions. The bottom boundary layer is represented by the linearized Navier-Stokes equations under the usual boundary layer approximation. It is found that the boundary layer velocity distribution and shear stress can be greatly altered from impermeable bed predictions. Theoretical results for energy dissipation and shear stress are compared to existing data and are found to agree very well. The predictions of classical small-amplitude wave theory are not appreciably modified away from the boundary.

1. Introduction

As ocean waves propagate away from their generation areas, they eventually encounter the coastal zone and, subsequently, sediments which constitute a loose bottom boundary to the wave motion. Komar *et al.* (1972) have photographed deep-water oscillatory ripple marks off the Oregon coast at depths of 200 m. It is therefore quite possible for a wave to have considerable interplay with the bottom before reaching the beach. This is especially true along wide continental shelves. From this point of view, wave-bottom interaction becomes of great practical importance to the activities of man. The design of coastal structures and port facilities as well as the management of navigable waterways are functions of predicted wave parameters and sediment transport.

Over the years, many studies of wave propagation over porous beds have been made. The first group of significant works were those of Putnam (1949) and Reid and Kajiura (1957). In those pioneer works the problem of wave-induced motions in the bottom sediment and the contribution to wave damping by such motions were basically solved. However, the inviscid model of the fluid motion used in both studies left an undesirable discontinuity at the water sediment interface, and also failed to account for all of the dissipation of the wave energy.

Subsequently, Hunt (1959) introduced viscosity in both the fluid and porous regions and applied a no-slip condition at the interface boundary. This condition upon the horizontal velocity was proven to be incorrect by Murray (1965) who invoked the arguments of the kinematic conservation of mass and the dynamic conservation of power. While the boundary conditions used by Murray (1965) did represent a major im-

[1] Present affiliation: Remote Sensing Branch, Naval Research Laboratory, Washington, D.C. 20375.

provement over the previous works, they were not as realistic as the model discussed by Beavers and Joseph (1967). The condition implemented by them allows for slippage of the tangential velocity component and is stated as

$$\frac{\partial u}{\partial z}=\frac{\alpha}{K^{\frac{1}{2}}}(u-\bar{u}_s) \quad \text{at} \quad z=0, \tag{1}$$

where K is the permeability, u the tangential velocity, $\bar{u}_s$ the porous bed flow as given by Darcy's law and α a constant whose value depends on the local porosity. Slip-boundary conditions of similar form have been used in slightly rarefied gas problems (Eckert and Drake, 1959), but Beavers and Joseph have adapted the concept for high density fluid flow over porous boundaries with internal parallel flow. They performed a series of experiments to determine some values of α and to confirm the validity of the model. Recently, additional papers by Taylor (1971) and Richardson (1971) experimentally and theoretically confirmed the applicability of the condition to such problems.

The condition stated in (1) is similar in form to the "radiation-type" boundary condition found in other physical problems such as heat conduction (Luikov, 1968). In the present case, it is essentially a statement concerning the interaction of the shear stress distribution across the interface and the boundary flow condition. Since the shear stress is a controlling parameter in determining the incipient motion and the subsequent sediment transport as discussed by Yang (1973), Francis (1973) and Komar and Miller (1975), it is necessary to study the detailed motion at the interface with the correct boundary conditions. Since the condition used here deals specifically with the stress distribution, the results can be used to clarify unsettled problems regarding both the shear stress and its relationship to sediment motion. For example, Liu's (1973) work assumed the shear stress to be continuous across the interface while we allow it to be discontinuous. This difference should have important effects on any analytical derivation of threshold conditions.

Thus, the purpose of this paper is to utilize the condition (1) in order to investigate the effect of the porous bed on the propagation of linear waves and to enhance our understanding of wave-bottom interactions. In the analysis, a large number of assumptions are made which may limit practical application to a certain extent, but judicious deletion of particular terms in the equations of motion allows analytic solution of the coupled problem and clarifies the influence of the boundary condition.

2. Theoretical analysis

a. Equations of motion

The problem of wave propagation over a porous bed involves flow in two distinct regions, i.e., the fluid and the porous bed as shown in Fig. 1. The interior

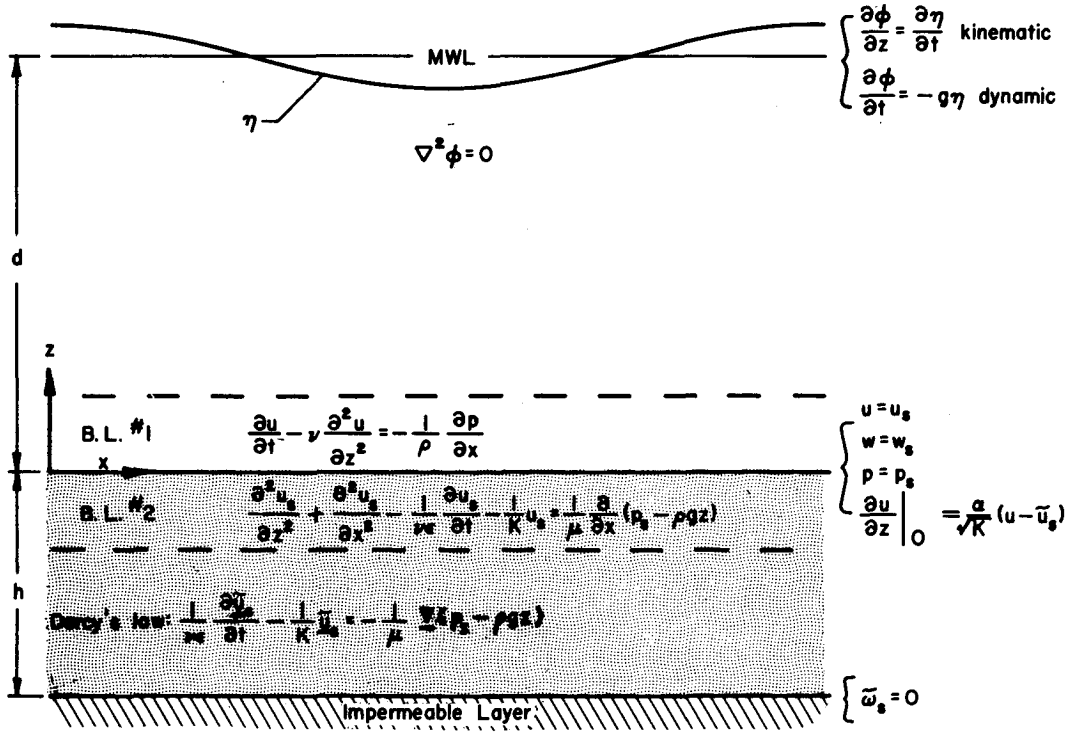

FIG. 1. Equations of motion and boundary conditions.

flow in the fluid regime is assumed to be irrotational. Thus the motion is governed by Laplace's equation

$$\nabla^2\phi=0, \tag{2}$$

with ϕ as the velocity potential function. Viscous effects have thus been assumed negligible in the interior regime; the density is assumed to be constant and gravity is the only body force considered. The flow in the porous bed is governed by Darcy's law

$$\frac{\rho}{\mu\epsilon}\frac{\partial\tilde{\mathbf{u}}_s}{\partial t}+\frac{1}{K}\tilde{\mathbf{u}}_s=-\frac{1}{\mu}\nabla(p_s-\rho gz), \tag{3}$$

where ϵ is the porosity, K the specific permeability, $\tilde{\mathbf{u}}_s$ the seepage velocity, μ the dynamic viscosity, ρ the density and p_s the pressure, with the subscript s indicating the quantities in the porous region.

Since the transition between the fluid and the porous regions is rather drastic, the shear stress will be strong locally and the viscous effect cannot be neglected. Two boundary layers are introduced to couple the flows in the two regions as shown in Fig. 1. In boundary layer 1 on the fluid side, the boundary layer equation used is

$$\frac{\partial u}{\partial t}-\nu\frac{\partial^2 u}{\partial z^2}=-\frac{1}{\rho}\frac{\partial p}{\partial x}. \tag{4}$$

The momentum equation utilized in boundary layer 2 is a result derived by Brinkman (1947) for a field of closely packed spheres. This equation has been discussed by Batchelor (1974) and is expressed as

$$\frac{\partial^2 u_s}{\partial z^2}+\frac{\partial^2 u_s}{\partial x^2}-\frac{1}{\nu\epsilon}\frac{\partial u_s}{\partial t}-\frac{1}{K}u_s=-\frac{1}{\mu}\frac{\partial}{\partial x}(p_s-\rho gz), \tag{5}$$

in the horizontal. The vertical equation has a similar form with the differentiation of the pressure term being with respect to z rather than x.

b. Boundary conditions

Boundary conditions will now be proposed so that the wave, porous bed problem can be addressed in a completely well-posed sense.

At the free surface, the linearized kinematic and dynamic boundary conditions are

$$\frac{\partial\phi}{\partial z}=\frac{\partial\eta}{\partial t}, \tag{6}$$

$$\frac{\partial\phi}{\partial t}=-g\eta, \tag{7}$$

where η represents the surface displacement measured from the mean water level.

At the bottom of the porous bed, the vertical velocity is taken to be zero, i.e.,

$$\tilde{w}_s=0. \tag{8}$$

A few words of explanation are needed here. Strictly speaking, at the bottom of the porous bed, there should be another boundary layer similar to boundary layer 2. However, the velocity will be extremely slow at this boundary so its influence is considered negligible. As a result, the only condition needed here is the condition outside the boundary, i.e., the vanishing of the vertical velocity component.

The most important set of boundary conditions is at the fluid, porous bed interface, where the equations of motion will be matched. The matching conditions are

$$u=u_s, \tag{9}$$

$$w=w_s, \tag{10}$$

$$p=p_s, \tag{11}$$

$$\left.\frac{\partial u}{\partial z}\right|_0=\frac{\alpha}{K^{\frac{1}{2}}}(u-\tilde{u}_s)|_0. \tag{12}$$

Eqs. (9)–(11) state the continuity of velocity and pressure, while (12) states the new radiation-type boundary condition.

c. The solutions

As discussed in Section 1b and shown in Fig. 1, the problem includes four regions each of which is governed by differential equations. The route taken in order to solve these four coupled equations is determined by the radiation condition and the continuity of horizontal velocity condition. To begin, the solution to Laplace's equation in the fluid regime is found. Next, we proceed to the porous bed and derive the solution to Darcy's equation. At this point, the terms in the radiation condition are available and the flow field in boundary layer 1 can be found subject to the radiation condition. Finally, the flow in boundary layer 2 is derived satisfying the continuity of horizontal flow. This procedure results in five linear expressions in five unknowns. The system is solved and used to determine the sixth integration constant. These values are listed in Table 1.

Since the motion of interest consists of a train of waves represented by

$$\eta=ae^{i\chi}, \tag{13}$$

the solution sought is periodic and therefore ϕ is assumed to be

$$\phi=(A_1\cosh kz+B_1\sinh kz)e^{i\chi}, \tag{14}$$

where $\chi=kx-\sigma t$, x is the horizontal coordinate and the wave is propagating in the positive x direction.

Substituting ϕ and η into (6) yields the following

TABLE 1. Values of the constants of integration.

1. $$\text{Det}\,\bar{A}=2k\cosh kh\left\{\left[\frac{\alpha}{\sqrt{K}}+(1-i)b-k^2\left(\frac{1}{(1-i)b}+\frac{1}{\theta}\right)\right]+\coth kd\left[\frac{(1-i)b}{\theta}-\frac{\alpha}{\sqrt{K}(1-i)b}\right]\left(k+\frac{\lambda\sigma}{\nu}\right)\right\}$$
$$-\frac{2\lambda\sigma}{\nu}\left[\frac{\alpha}{\sqrt{K}}+(1-i)b\right]\coth kd\,\sinh kh$$

2. $$A_1\cdot\text{Det}\,\bar{A}=\frac{2a\sigma i}{\sinh kd}\left\{k^2\left[\frac{1}{(1-i)b}+\frac{1}{\theta}\right]-\left[\frac{\alpha}{\sqrt{K}}+(1-i)b\right]\right\}\cosh kh$$

3. $$B_1\cdot\text{Det}\,\bar{A}=\frac{2a\sigma^2 i}{\nu\sinh kd}\left\{\left(\lambda+\frac{\nu k}{\sigma}\right)\left[\frac{\alpha}{\sqrt{K}(1-i)b}-\frac{(1-i)b}{\theta}\right]\cosh kh+\frac{\lambda}{k}\left[\frac{\alpha}{\sqrt{K}}+(1-i)b\right]\sinh kh\right\}$$

4. $$A_1'\cdot\text{Det}\,\bar{A}=\frac{2a\sigma^2}{\nu\sinh kd}\left[\left(\frac{k^2\lambda}{\theta}-\frac{\lambda\alpha}{\sqrt{K}}-\frac{\alpha\nu k}{\sigma\sqrt{K}}+\frac{k^3\nu}{\sigma\theta}\right)\cosh kh-k\lambda\sinh kh\right]$$

5. $$\frac{A_2\cdot\text{Det}\,\bar{A}}{e^{kh}}=\frac{B_2\cdot\text{Det}\,\bar{A}}{e^{-kh}}=\frac{-a\sigma^2}{\nu\sinh kd}\left[\frac{\alpha}{\sqrt{K}}+(1-i)b-\frac{k^2}{(1-i)b}-\frac{k^2}{\theta}\right]$$

6. $$A_2'\cdot\text{Det}\,\bar{A}=\left\{\left[\frac{a\lambda\sigma^2}{\nu}\left(\frac{k^2}{\theta}-\frac{\alpha}{\sqrt{K}}\right)+\left(2k+\frac{\sigma\lambda}{\nu}\right)\left(a\sigma(1-i)b-\frac{a\sigma k^2}{(1-i)b}\right)\right]\frac{\cosh kh}{\sinh kd}-\frac{2a\sigma^2 k\lambda\sinh kh}{\nu\sinh kd}\right\}$$

$$b=(\sigma/2\nu)^{\frac{1}{2}},\quad \lambda=\frac{ikK\nu\epsilon}{(\nu\epsilon-iK\sigma)},\quad \theta=\left(\frac{1}{K}-\frac{i\sigma}{\nu\epsilon}\right)^{\frac{1}{2}}$$

relation between the integration constants:

$$A_1+B_1\coth kd=\frac{-ia\sigma}{k\sinh kd}. \tag{15}$$

The condition at the bottom is that the horizontal and vertical velocity components are continuous. The conditions cannot be applied until the general solutions for the bed flow and boundary layer motions are obtained, since the flows are coupled. Expressions for U and W can be obtained by differentiating ϕ with respect to x and z, respectively, i.e.,

$$U=ik(A_1\cosh kz+B_1\sinh kz)e^{ix} \tag{16}$$

$$W=k(A_1\sinh kz+B_1\cosh kz)e^{ix}. \tag{17}$$

The pressure is related to ϕ using the linearized Bernoulli equation

$$p=-\rho\frac{\partial\phi}{\partial t}+\rho g(z-d) \tag{18}$$

or

$$p=i\rho\sigma(A_1\cosh kz+B_1\sinh kz)e^{ix}+\rho(z-d)g, \tag{19}$$

where ρ is the fluid density and g the acceleration of gravity.

Now we will attend to the porous bed flow. Darcy's law, as stated in (3), is solved as a potential flow problem (Polubarinova-Kochina, 1962) using the relations

$$\frac{1}{\nu\epsilon}\frac{\partial\tilde{u}_s}{\partial t}+\frac{1}{K}\tilde{u}_s=-\frac{1}{\mu}\frac{\partial}{\partial x}(p_s-\rho gz)=U_s, \tag{20}$$

$$\frac{1}{\nu\epsilon}\frac{\partial\tilde{w}_s}{\partial t}+\frac{1}{K}\tilde{w}_s=-\frac{1}{\mu}\frac{\partial}{\partial z}(p_s-\rho gz)=W_s, \tag{21}$$

where ν is the kinematic viscosity. Since continuity must also apply to the bed, $\partial\tilde{u}_s/\partial x+\partial\tilde{w}_s/\partial z=0$. It follows that $\partial U_s/\partial x+\partial W_s/\partial z=0$. From (20) and (21), it is seen that U_s and W_s are expressed as the gradient of a function. Therefore, let

$$U_s=\frac{\partial\phi_s}{\partial x}\quad\text{and}\quad W_s=\frac{\partial\phi_s}{\partial z}. \tag{22}$$

Substitution of (22) into the continuity equation implies $\nabla^2\phi_s=0$. Substituting (22) into (20) and integrating over x, we find

$$\phi_s=-(1/\mu)(p_s-\rho gz)+D_2. \tag{23}$$

If we let

$$\phi_s=(A_2e^{kz}+B_2e^{-kz})e^{ix}+G(z), \tag{24}$$

then from Laplace's equation,

$$G(z)=C'z+D'. \tag{25}$$

The condition at $z=0$ to be satisfied by this flow is continuity of pressure, so the potential pressure field is assumed to be undiminished across the boundary layer. To prove this point, the vertical momentum equation must be considered since it contains the $\partial p/\partial z$ term. The usual approach (Schlichting, 1968) is to nondimensionalize the momentum equations and show that all the terms in the z equation which contain w are small compared with the terms in the x equation. If this is so, $\partial p/\partial z$ equals the sum of a

number of small terms and is therefore small itself. In this case the situation is somewhat different since percolation across the interface is allowed. However, the seepage velocity is determined by the ratio, K/μ, which has a maximum value of 10^{-3} cm^3 s g^{-1}. The increase in w at the interface over the value of zero for the impermeable case remains small compared to U_0 and the standard boundary layer approximations remain valid. (Note that the subscript 0 denotes evaluation at $z=0$.) Thus

$$\phi_s|_0=(A_2+B_2)e^{i\chi}+D'=p_s|_0, \tag{26}$$

$$p_s|_0=(-i\sigma A_1/\nu)e^{i\chi}+(gd/\nu)+D_2. \tag{27}$$

Relations (26) and (27) then give

$$A_2+B_2=-i\sigma A_1/\nu, \tag{28}$$

$$D'=(gd/\nu)+D_2. \tag{29}$$

In order to apply the boundary condition at $z=-h$, an expression for $\tilde{w}_s$ must be obtained. This is achieved by solving (21), rewritten as

$$\tilde{w}_s=\left[(w_s)_i+\nu\epsilon\int_0^t e^{\nu\epsilon t/K}\left(\frac{\partial\phi_s}{\partial z}\right)dt\right]e^{-\nu\epsilon t/K}. \tag{30}$$

If we assume that the motion is initially zero, $(\tilde{w}_s)_i$ can be dropped. Performing the integration results in the following expression for $\tilde{w}_s$:

$$\tilde{w}_s=\frac{k\nu\epsilon K}{(\nu\epsilon-i\sigma K)}(A_2e^{kz}-B_2e^{-kz})e^{i\chi}+\mathrm{K}C'. \tag{31}$$

The condition at $z=-h$ is $\tilde{w}_s=0$. Application of this condition results in the two expressions

$$A_2e^{-kh}-B_2e^{kh}=0, \tag{32}$$

$$C'=0. \tag{33}$$

From (23)–(25) and (29), it is found that

$$p_s=-\mu(A_2e^{kz}+B_2e^{-kz})e^{i\chi}+\rho g(z-d), \tag{34}$$

and from continuity, one finds that

$$\tilde{u}_s=\frac{ik\nu\epsilon K}{(\nu\epsilon-i\sigma K)}(A_2e^{kz}+B_2e^{-kz})e^{i\chi}. \tag{35}$$

At this point, we return to the fluid regime and solve the boundary layer equations.

As discussed in the previous section, a linearized laminar boundary layer is assumed for boundary layer 1. The criteria for this assumption is strongly dependent on the expansion parameter $\hat{\epsilon}$ and will be discussed further once the solutions are obtained. The x-momentum equation is

$$\frac{\partial u}{\partial t}-\nu\frac{\partial^2 u}{\partial z^2}=-\frac{1}{\rho}\frac{\partial p}{\partial x}=\frac{\partial^2\phi}{\partial x\partial t}. \tag{36}$$

Now if $u=\partial\phi/\partial x+u'$, then (36) becomes

$$\frac{\partial u'}{\partial t}-\nu\frac{\partial^2 u'}{\partial z^2}=0. \tag{37}$$

[The decomposition of u into a potential component plus a viscous correction term u' is discussed in Phillips (1969).] As z increases away from the interface, viscous effects decrease to an insignificant amount implying that u' approaches zero so the solution to (37) becomes

$$u'=A_1'\exp[(i-1)bz+i\chi], \tag{38}$$

where

$$b=+(\sigma/2\nu)^{\frac{1}{2}}.$$

The condition at $z=0$ is the radiation-type condition described in (12). When the decomposition of u is employed, then

$$\frac{\partial u'}{\partial z}=\frac{\alpha}{K^{\frac{1}{2}}}(u'+U-\tilde{u}_s)-\frac{\partial U}{\partial z}\quad\text{at}\quad z=0. \tag{39}$$

Substituting the expressions for u', $\tilde{u}_s$ and U into (39) and evaluating at $z=0$ yields the condition

$$\frac{ik\alpha}{K^{\frac{1}{2}}}A_1-ik^2B_1+\left[\frac{\alpha}{K^{\frac{1}{2}}}+(1-i)b\right]A_1'-\frac{\lambda\alpha}{K^{\frac{1}{2}}}(A_2+B_2)=0, \tag{40}$$

where $\lambda=ik\nu\epsilon K/(\nu\epsilon-i\sigma K)$. An expression for w',

$$w'=\frac{iku'}{(1-i)b}, \tag{41}$$

can be obtained from continuity.

One of the implications involved with the radiation-type boundary condition at $z=0$ is that viscous effects diffuse at least a small distance into the bed. The extent of this viscous penetration depends on the permeability and porosity. Although this distance is probably very small for the bed materials under consideration, the effect on the shear stress may prove to be significant. Since shear stress is related to the horizontal velocity, an additional condition must be imposed to make the problem well-posed. In the present analysis, the continuity of horizontal velocity is chosen instead of stress. Physically, a jump condition in velocity implies either nonconservation of mass or infinite local shear stress. Neither choice sounds reasonable. On the other hand, the choice of continuity of horizontal velocity can avoid all the above difficulties. This choice does lead to a jump in the shear stress across the interface, but physically this discontinuity in shear stress is a statement of finite

shear stress bearing capability of the sediment. Furthermore, the matching of the horizontal velocity at the interface is consistent with the idealized bed flow. Introduction of this matching layer is also necessary mathematically since both A_2 and B_2 have been utilized in (28) and (32). The matching layer adds another integration constant which makes the total number of constants equal to the number of boundary conditions (not including the dynamic surface condition). As in boundary layer 1, viscous effects decrease away from the interface and approach zero at some distance away from the bottom.

The equation used for boundary layer 2 is given in (5) with $\partial^2 u_s/\partial x^2$ dropped for the same reasons applied in boundary layer 1. If u_s is decomposed in the same manner as u, i.e., $u_s=\bar{u}_s+u_s'$, Eq. (5) becomes

$$\frac{\partial^2 u_s'}{\partial z^2}-\frac{1}{\nu\epsilon}\frac{\partial u_s'}{\partial t}-\frac{1}{K}u_s'=0. \tag{42}$$

The condition to be satisfied at $z=0$ is

$$u_s'=U+u'-\bar{u}_s. \tag{43}$$

As with boundary layer 1, a solution can be obtained in the form of

$$u_s'=A_2' e^{\theta z+i\chi}. \tag{44}$$

Upon making this substitution and solving for θ,

$$\theta=\left(\frac{1}{K}-\frac{i\sigma}{\nu\epsilon}\right)^{\frac{1}{2}}. \tag{45}$$

From (43) it is found that

$$A_2=ikA_1+A_1'-\lambda(A_2+B_2). \tag{46}$$

Using the continuity equation

$$w_s'=\frac{-iku_s'}{\theta}, \tag{47}$$

which allows the last remaining condition, that of a continuous mass flux across the interface, to be satisfied. This condition is expressed as either

$$W_0+w_0'-\bar{w}_s|_0-w_s'|_0=0 \tag{48}$$

or

$$-\frac{k^2}{\theta}A_1+kB_1+ik\left(\frac{1}{\theta}+\frac{1}{(1-i)b}\right)A_1'+i\lambda\left(1-\frac{k}{\theta}\right)A_2-i\lambda\left(1+\frac{k}{\theta}\right)B_2=0. \tag{49}$$

Conditions (15), (28), (32), (40) and (49) supply the information needed to find the values of A_1, B_1, A_2, B_2 and A_1', which are the only remaining constants found in the expressions for the various velocity components. The values of these constants are listed in Table 1 where $\bar{A}$ represents the augmented coefficient matrix.

3. Discussion

Knowing the solutions and the integration constants, it is now possible to derive expressions for the physical quantities of interest. As seen in Table 1, the integration constants are quite lengthy and contain real and imaginary components. For natural conditions, quite a number of simplifications can be made with the establishment of the appropriate criteria based on the values of the physical parameters involved. In the following derivations, the calculations are usually long involving much algebra. It serves no purpose to reproduce them here. The procedure in all derivations is to find the quantity in terms of the simplified forms of A_1, B_1, A_1', A_2 and B_2, separate the real from the imaginary components and finally simplify that result. The values of $\alpha/K^{\frac{1}{2}}$ used in the sample calculations were selected to be of similar order as those given in Joseph and Beavers' experiments. It is acknowledged that their beds were artificial although the permeabilities were equivalent to those of oceanic sand beds.

The velocity potential ϕ is found to be essentially the same as given by Airy wave theory for natural conditions, i.e.,

$$\phi=\frac{a\sigma}{k}\left[\frac{\cosh kz\,\sin\chi}{\sinh kd}-(J^2+I^2)^{\frac{1}{2}}\times\frac{\sigma K^{\frac{1}{2}}\,\mathrm{sech}kh}{\alpha\nu\xi\sinh kd}\sinh kz\,\sin(\chi+\Theta^*+\psi)\right], \tag{50}$$

where

$$I=-\{(\alpha k\nu/2bK^{\frac{1}{2}}\sigma)\cosh kh+K[(\sigma/K^{\frac{1}{2}})+b]\sinh kd\},$$

$$J=-[(\sigma k\nu/2bK^{\frac{1}{2}}\sigma)\cosh kh+Kb\sinh kh],$$

$$\xi=[1+(2bK^{\frac{1}{2}}/\alpha)+2(b/\alpha)^2K]^{\frac{1}{2}},$$

$$\theta^*=\tan^{-1}[b/(\alpha/K^{\frac{1}{2}}+b)],$$

$$\psi=\tan^{-1}(I/J)=a\tan(|I|/|J|)+\pi.$$

Note that the $\sinh kz$ term is due to the porous bed modification of ϕ and approaches the value zero as $z\to 0$. The horizontal and vertical potential velocities can be obtained by differentiating ϕ with respect to x and z, respectively. The ratio of the first term to the second term of ϕ can be shown to be of the order of $b/k\approx L/\delta\gg 1$. For this reason, and also the fact that the second term of ϕ vanishes at $z=0$, the expression for U is approximately

$$U=\frac{a\sigma\cosh kz}{\sinh kd}\cos\chi. \tag{51}$$

Since the vertical velocity at $z=0$ is of interest the minor term of ϕ will not be dropped from W, and

$$W=a\sigma\left[\frac{\sinh kz}{\sinh kd}\sin\chi-(J^2+I^2)^{\frac{1}{2}}\times\left(\frac{\sigma K^{\frac{1}{2}}\operatorname{sech}kh}{\alpha\nu\xi\sinh kd}\right)\cosh kz\sin(\chi+\Theta^*+\psi)\right]. \quad (52)$$

To this approximation, the pressure distribution remains unaffected by the porous bed since ϕ is virtually the same as in the impermeable bed case. The pressure is written as $p=-\rho\phi_t+\rho g(z-d)$ or

$$p=\rho\frac{a\sigma^2\cosh kz}{k\sinh kd}\cos\chi+\rho g(z-d). \quad (53)$$

This result agrees with that of Putnam (1949), who left the bed and fluid motions uncoupled and simply used the pressure field of an Airy wave to drive the bed flow.

Now that an expression for ϕ has been obtained, the value of $\hat{\epsilon}\approx\phi_x^2/\phi_t\approx ak$. Therefore, this wave theory is valid for $ak\ll 1$ and under this circumstance the dropping of the nonlinear terms in the surface boundary conditions and the boundary layer equation is justified.

The value of ϕ_s is the same as Putnam's (1949), notwithstanding an error which was corrected by Reid and Kajiura (1957):

$$\phi_s=\frac{-a\sigma^2\cosh k(z+h)\cos\chi}{\nu k\sinh kd\cosh kh}+\frac{gd}{\nu}. \quad (54)$$

Expressions for p_s, $\tilde{u}_s$ and $\tilde{w}_s$ are, respectively,

$$p_s=\frac{\rho a\sigma^2\cosh k(z+h)\cos\chi}{k\sinh kd\cosh kh}+\rho g(z-d), \quad (55)$$

$$\tilde{u}_s=\frac{a\sigma^2K\cosh k(z+h)\sin\chi}{\nu\sinh kd\cosh kh}, \quad (56)$$

$$\tilde{w}_s=\frac{-a\sigma^2K\sinh k(z+h)\cos\chi}{\nu\sinh kd\cosh kh}. \quad (57)$$

(The reader should recall that z is negative in the bed.)

Inside boundary layer 1, the result for u' is

$$u'=-\frac{a\sigma e^{-bz}}{\xi\sinh kd}\cos(\chi+bz+\Theta^*). \quad (58)$$

Since a decrease in $\alpha/K^{\frac{1}{2}}$ indicates less resistance to the boundary layer flow as seen from the boundary condition, it will affect a decrease in u'. Therefore $u=U+u'$ increases in magnitude as does the phase advance Θ^* because U and u' have opposite signs. Within this boundary layer

$$w'=\frac{a\sigma ke^{-bz}}{\sqrt{2}\xi b\sinh kd}\cos(\chi+bz+\Theta^*-\pi/4). \quad (59)$$

Comparing w' to u', it is seen that u' is greater by a factor of approximately L/δ.

Figs. 2 and 3 show the boundary layer profiles for two different values of $\alpha/K^{\frac{1}{2}}$. There is an appreciable difference between the two examples in the lower

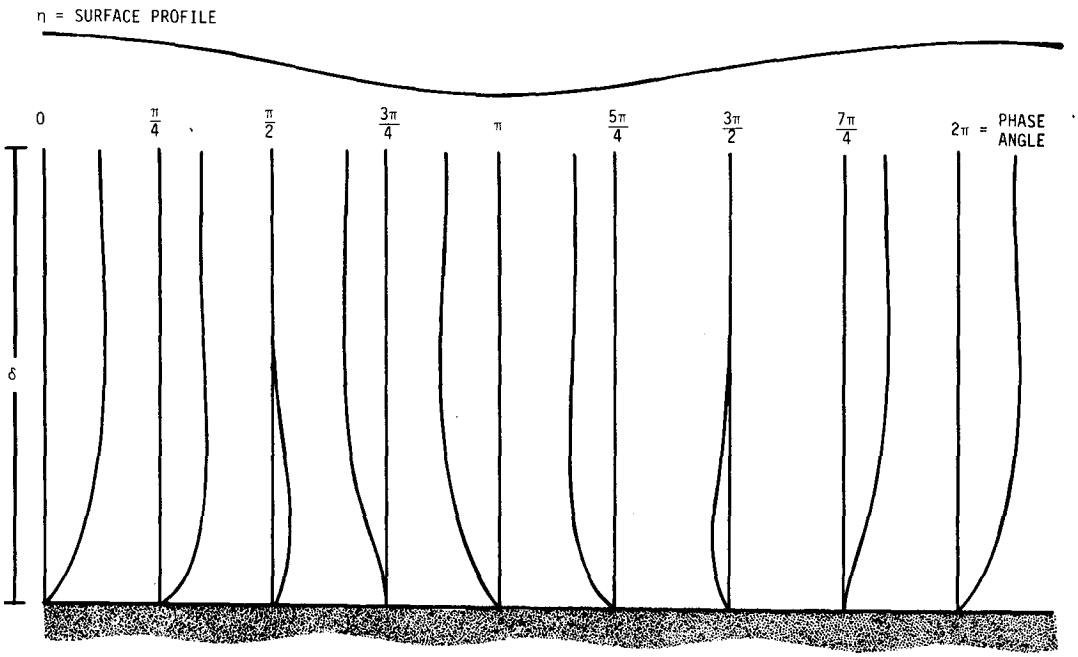

FIG. 2. Boundary layer profiles of u/U_0, period=8 s for $\alpha/K^{\frac{1}{2}}=100$ cm^{-1}, $\nu=0.01$ cm^2 s^{-1} ($U_0=a\sigma/\sinh kd$=maximum bottom velocity predicted by potential theory).

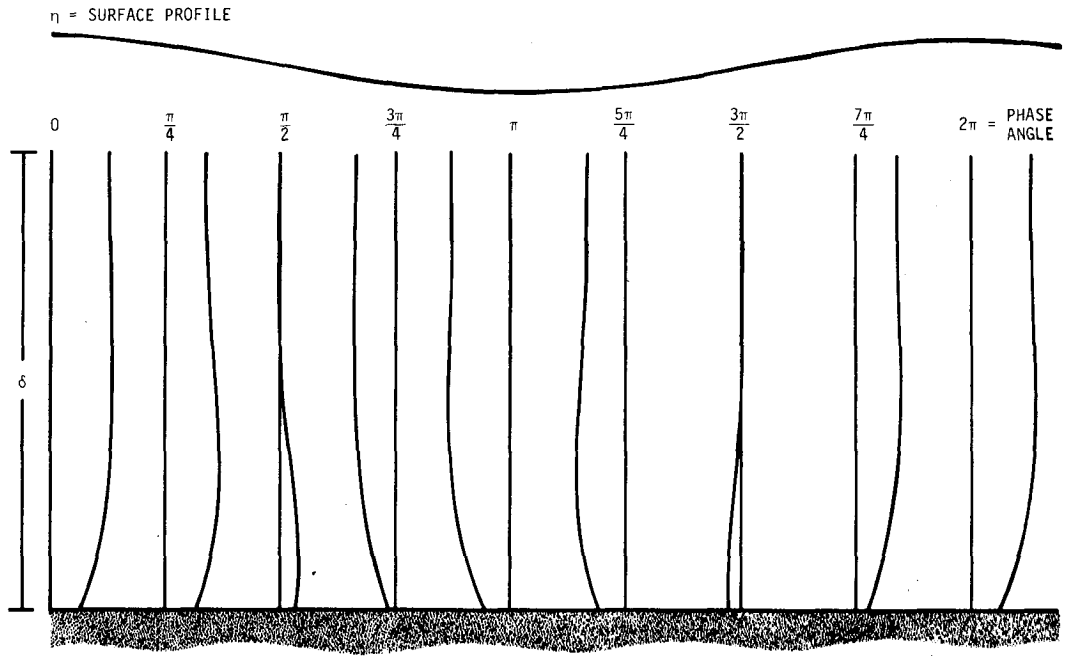

FIG. 3. As in Fig. 2 except for $\alpha/K^{\frac{1}{2}}=10$ cm^{-1}.

section of the layer. Note the value of u_0. To illustrate another trend, Fig. 4 plots u_0/U_0 over a wave period ($U_0=a\sigma/\sinh kd$). Finally, Fig. 5 shows the dependence of u_0 on the phase angle χ. As $\alpha/K^{\frac{1}{2}}$ decreases, there is a steady phase advance which can be substantial for small values of $\alpha/K^{\frac{1}{2}}$.

The boundary layer thickness is a function of a period [$\delta\propto(2\nu/\sigma)^{\frac{1}{2}}$]. Fig. 6 shows that for short-period waves $\delta\approx 0.5$–1.0 cm, and for boundary layer 2, $\delta_2\propto K^{\frac{1}{2}}\leqslant 10^{-3}$ cm. It is very difficult to assess the importance of the boundary layer other than that of mathematical necessity. Physically, this layer is so thin for ordinary porous beds that its thickness is merely a fraction of the grain diameter. It has been noted by several investigators (Murray, 1965) that the bed can become substantially fluidized near the interface before significant motion occurs, i.e., the bed reaches a "quick" state. If this is so, then the permeability will be greatly increased and the layer will extend deeper into the bed, thereby encompassing at least the first grain layer. There is another difficulty related to the problem of determining the thickness of the boundary, that of finding a definite value of effective permeability under dynamic conditions. Established procedures are by static tests. Therefore, the permeability is a material property. If the quick state observed is a rule, a new dynamic permeability should be defined as a function of both material properties and flow conditions. Such a development is clearly beyond the scope of the present study. We are concentrating here on the effect of the radiation condition.

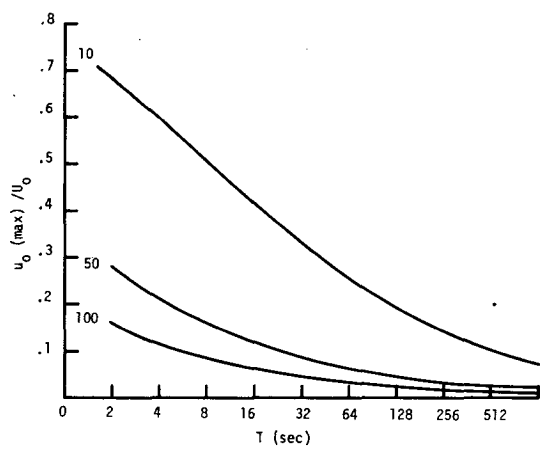

FIG. 4. Variation of $u_0(\max)/U_0$ with wave period. Curves represent constant values of $\alpha/K^{\frac{1}{2}}$ (cm^{-1}) for $\nu=0.01$ cm^2 s^{-1}.

One of the effects of the finite slip would be to decrease the surface shear stress, but increase the form drag of the interstitial flow on the particles. The correction velocity in layer 2 is

$$u_s'=[a\sigma\exp(z/K^{\frac{1}{2}})/\sinh kd][\cos\chi-\xi^{-1}\cos(\chi+\theta^*)] \quad \text{for } z\leqslant 0. \quad (60)$$

Unlike its counterpart u', u_s' has no depth-dependent phase. An example of the velocity profile across boundary layer 2 is shown in Fig. 7. Note that the negative scale is amplified in order to emphasize the flow reversal within the bed.

In order to show the detailed flow pattern, the stream-function is used which is defined by

$$u=-\psi_z \quad \text{and} \quad w=\psi_x. \quad (61)$$

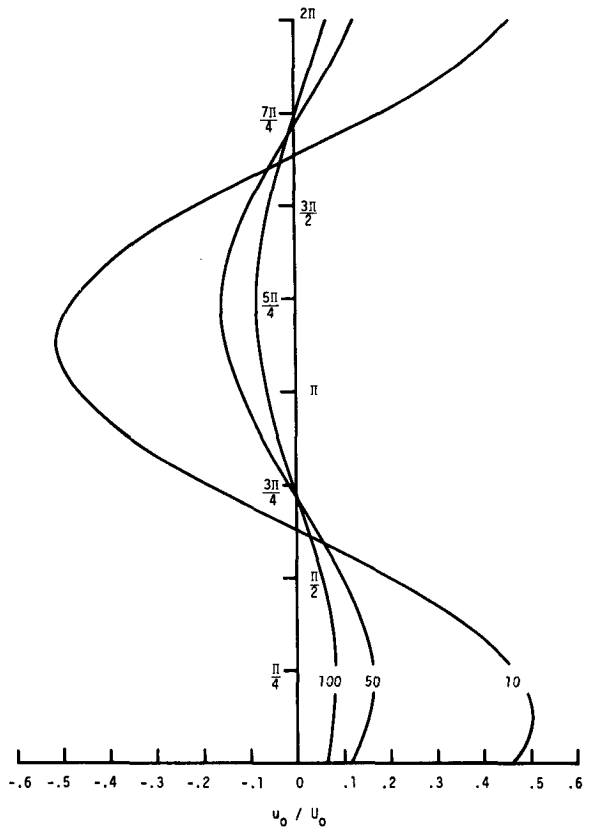

FIG. 5. Curves of relative bottom velocity versus phase angle for values of $\alpha/K^{\frac{1}{2}}$ (cm^{-1}): $T=8$ s, $\nu=0.01$ cm^2 s^{-1}.

The streamfunction in both the major flow regions is modified near the interface by ψ' which corresponds to u'. The streamfunction can be found by utilizing (16) and (17), and integrating (61), to obtain

$$\psi=\frac{a\sigma}{\sinh kd}\left[-\frac{\sinh kz}{k}\cos\chi+(J^2+I^2)^{\frac{1}{2}}\times\left(\frac{\sigma K^{\frac{1}{2}}\operatorname{sech}kh}{k\alpha\nu\xi}\right)\cosh kz\cos(\chi+\psi+\theta^*)\right]. \quad (62)$$

The second term represents a modification to the impermeable case. Its amplitude is small compared to the first term, except near the bottom where $\sinh kz\to 0$ and $\cosh kz\to 1$. Under the approximations applied, the value of the second term depends on b, the parameter arising from the boundary layer solution, and upon $\alpha/K^{\frac{1}{2}}$, the parameter given in the boundary condition. It also has a phase advance of $\sim\pi/4$ and derives its existence from the pumping action in the bed. As can be seen in Fig. 8, the streamlines in the bed intersect the interface in advance of the external flow.

The streamfunction for the porous bed flow is

$$\tilde{\psi}_s=\frac{-a\sigma^2K\sinh k(z+h)\sin\chi}{k\nu\sinh kd\cosh kh}, \quad (63)$$

which is 90° in advance of the potential field streamfunction.

The approximate corrections to the streamfunction in the boundary layers are given by

$$\psi'=\frac{-a\sigma e^{-bz}\cos(\chi+bz+\theta^*+\pi/4)}{2^{\frac{1}{2}}\xi b\sinh kd}, \quad (64)$$

$$\psi_s'=\frac{-a\sigma K^{\frac{1}{2}}\exp(z/K^{\frac{1}{2}})}{\sinh kd}[\cos\chi-\xi^{-1}\cos(\chi+\theta^*)]. \quad (65)$$

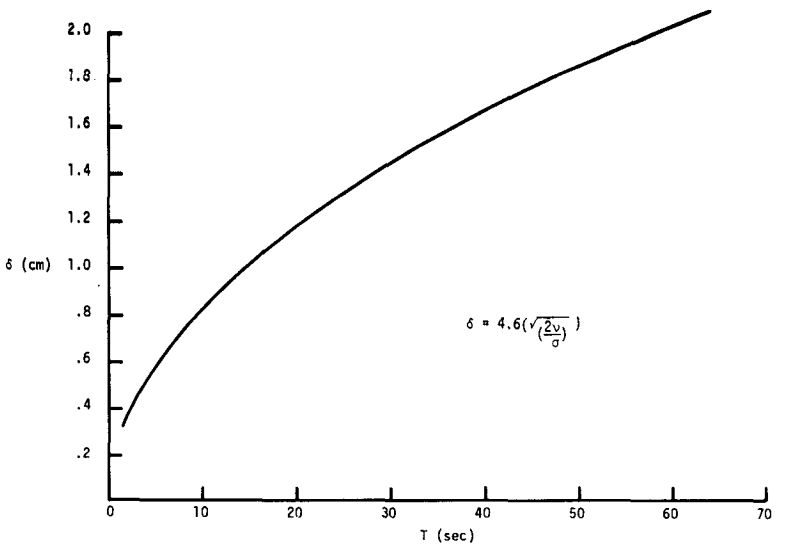

FIG. 6. Boundary layer thickness versus wave period.

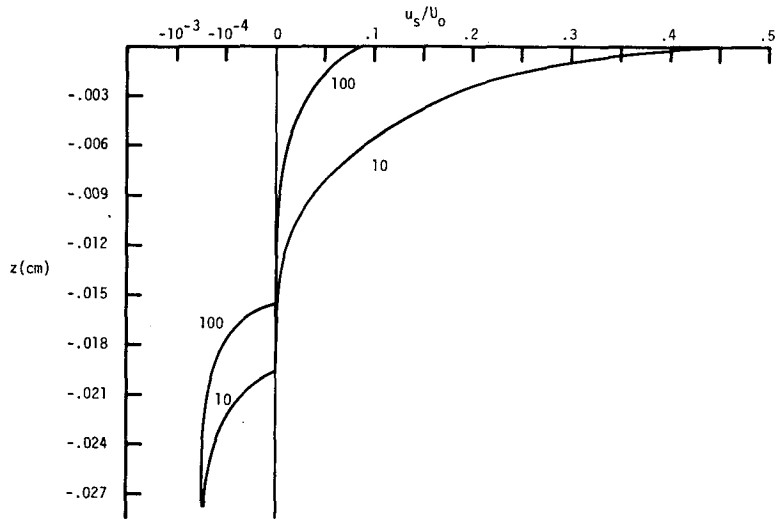

FIG. 7. Profiles of u_s/U_0 for different values of $\alpha/K^{\frac{1}{2}}$ (cm^{-1}): $T=8$ s, $K=10^{-5}$ cm^2, $h=7$ m, $\nu=0.01$ cm^2 s^{-1}.

The shear stress at the interface is the main cause of sediment motion. Fig. 9 shows the nondimensionalized shear stress with a representative number of measurements from Teleki and Anderson (1970). The quantity $\tau_0 \max/\rho U_0^2$ is proportional to the friction coefficient as stated in

$$c_f=\pi\tau_0/\rho U_0^2, \tag{66}$$

where n is a constant which must be determined experimentally. Unfortunately, all of Teleki and Anderson's data lie in what they considered to be the transition region $(35<U_0(2\nu/\sigma)^{\frac{1}{2}}\nu^{-1}<910)$. Also shown is the result from Kajiura's (1968) theory for C_f with $n=0.5$. Teleki and Anderson's data were collected using an impermeable sloping bottom (slope $=1:12.5$). Nonetheless, the theoretical curve shows a correct trend across the transition zone, and the theoretical value is smaller as expected both because of the presence of a porous bed, and because of the assumption of a laminar flow condition in the calculation. The bottom shear stress is given by

$$\tau_0=\frac{2^{\frac{1}{2}}\mu a\sigma b\cos(\chi+\theta^*-\pi/4)}{\xi\sinh kd}. \tag{67}$$

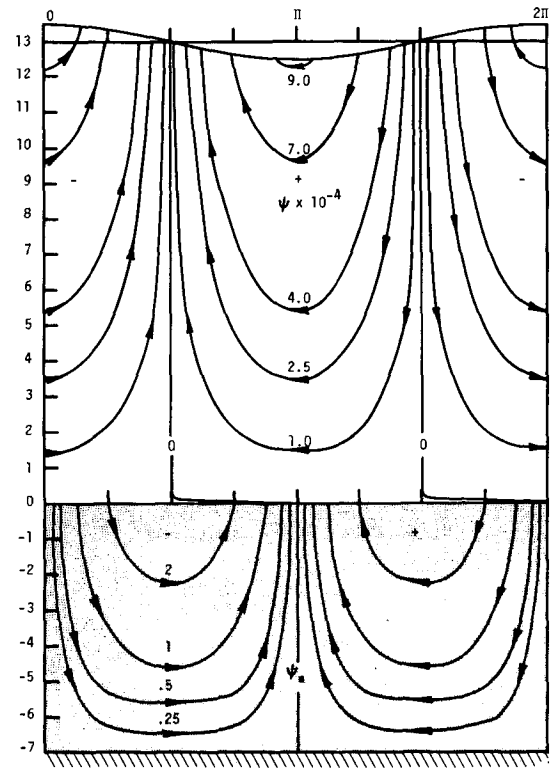

FIG. 8. Boundary layer streamlines: $L=100$ m, $d=13$ m, $h=7$ m, $a=1$ m, $K=10^{-6}$ cm^2, $\alpha/K^{\frac{1}{2}}=100$/cm, $\nu=0.01$ cm^2 s^{-1}.

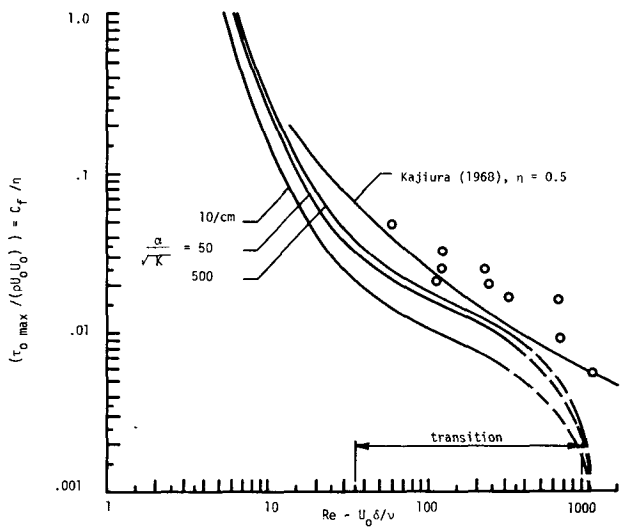

FIG. 9. Comparison of nondimensionalized bottom shear and data from Teleki and Anderson (1970).

Besides being useful in critical stress calculations, Eq. (67) could be used for critical stream power derivations as discussed by Bagnold (1963) and Yang (1973).

Energy dissipation occurs in all the regions. The values of d/L and h have the greatest effect on the relative importance of the energy loss in the three major regimes. To calculate the rate of loss in the fluid region, Rayleigh's dissipation function is employed (Rouse, 1961). Contributions will arise from the external flow and the boundary layer. Energy dissipation is given by

$$D=2\mu\int_0^L\int_0^d[u_x^2+w_z^2+\tfrac{1}{2}(u_z+w_x)^2]dzdx, \quad (68)$$

where major contributors to fluid domain losses are given by

$$D_1=4\mu\int_0^L\int_0^d[U_x^2+W_z^2]dzdx + \mu\int_0^L\int_0^\infty(u_z')^2dzdx. \quad (69)$$

Here the subscripts denote differentiation. The first term is due to the potential flow and the second is from the boundary layer. The first term is evaluated as

$$D_f=4\pi\mu a^2\sigma\coth kd, \quad (70)$$

an expression identical to Hough's (1896) result. The boundary layer loss is

$$D_{bl}=\tfrac{1}{2}\mu bL(a\sigma/\xi\sinh kd)^2. \quad (71)$$

The porous bed rate of loss is calculated in the same manner as in Putnam's (1949) determination, and is

$$D_{pb}=\frac{\mu}{K}\int_0^L\int_{-h}^0(\tilde{u}_s^2+\tilde{w}_s^2)dzdx = \frac{\rho K}{\pi\nu}\left(\frac{a\sigma^2L}{2\sinh kd}\right)^2\tanh kh. \quad (72)$$

This is exactly the same result as obtained by Reid and Kajiura (1957). Figs. 10 and 11 show the relative contributions of D_{bl} and D_{pb} for a typical wavelength in various depths of water and over beds of various thicknesses. Figs. 12 and 13 compare theoretical rates of energy loss to experimental values from Savage (1953). All of Savage's waves were intermediate waves, i.e., $1/20<d/L<1/2$.

The attenuation coefficient γ is defined as $D/2E$. The energy E of a small amplitude wave is $\rho ga^2L/2$. Since $D=-\dot{E}=-\rho gaa_tL$ and $a_x=a_t/C_g$, where C_g is the group velocity and equals the rate of energy

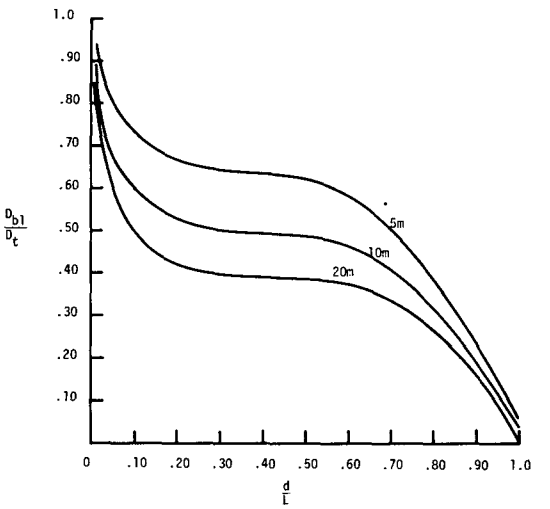

FIG. 10. Fractional dissipation due to boundary layer as a function of depth-to-wavelength ratio curves for various bed thicknesses: $L=100$ m, $K=10^{-6}$ cm^2, $\nu=0.01$ cm^2 s^{-1}, $\alpha/K^{\frac{1}{2}}=100$ cm^{-1}.

transmission in the wave, we have

$$a_x=\frac{-2\gamma E}{\rho gaC_gL}=\frac{-\gamma a}{C_g}.$$

Therefore,

$$a=a_ie^{-\gamma x/C_g}=a_ie^{-\gamma t}. \quad (73)$$

In evaluating the attenuation coefficient, the linearized group velocity is used because the changes of either group velocity or the phase velocity by the porous bed are negligible. A more complete treatment of the attenuation of the wave energy should follow the approach used by Reid and Kajiura (1957). In the present analysis, the emphasis is on the influence of the boundary conditions. Since the amplitude has been assumed to be constant to simplify the algebra, the results obtained in the analysis should be regarded

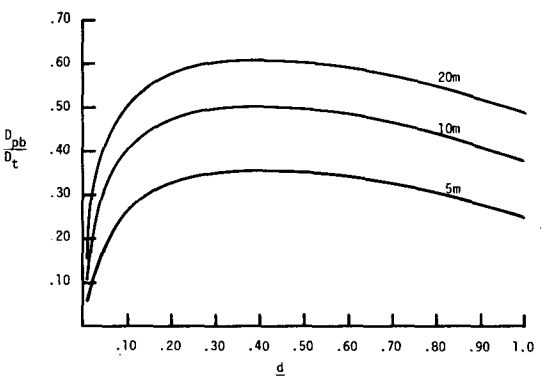

FIG. 11. Ratio of porous bed dissipation to total energy loss for various bed depths: $L=100$ m, $K=10^{-6}$ cm^2, $\alpha/K^{\frac{1}{2}}=100$ cm^{-1}, $\nu=0.01$ cm^2 s^{-1}.

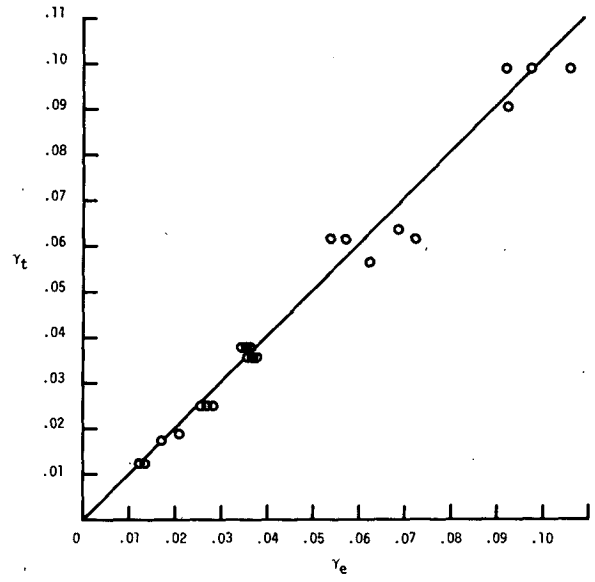

FIG. 12. Comparison of theoretical and experimental attenuation coefficients [data by Savage (1953)]: $\nu=0.01$ cm^2 s^{-1}, $\alpha/K^{\frac{1}{2}}=100$ cm^{-1}.

as local properties, i.e., the validity of the results is limited to a given neighborhood where the amplitude shows no substantial change. Improvement will be quite involved algebraically but relatively simple in principle.

The dispersion relationship can be derived from the unused boundary condition (7). The result of substituting (13) and (50) into (7) is approximately

$$\sigma^3\{(K/\nu)\tanh kh\exp[i(Y'+\theta^*)]\} -\sigma^2\operatorname{ctnh}kd+gk=0, \quad (74)$$

where $Y'=\tan^{-1}[1+\alpha/(bK^{\frac{1}{2}})]$. Since $\sigma K/\nu\approx 10^{-3}$, Eq. (74) reduces to the result predicted by Airy theory.

4. Conclusions

It has been shown that porous bed effects can produce significant adjustments in the structure of the bottom boundary layer. The results expressed here are subject to rather stringent restraints, i.e., the bottom boundary layer is laminar and the bed is stationary. Nonetheless, understanding of the laminar case is valuable to the understanding of the transition and turbulent flow regimes. Also, knowledge of the shear stress is a prerequisite to prediction of the threshold conditions. At present very little data exist on the boundary layer structure and the shear stress related to wave motion above a porous bed. Since the layer is typically very thin, measurements are difficult and new techniques need to be developed.

As for the radiation condition, for successful application to be accomplished, determination of α for natural bed materials is required. The properties of the bed at the interface may not be typical compared to the gross properties when pressure gradients and flow fields are present. If this is the case, the values of α, ϵ and K will be altered. The question of whether sediment motion is a sudden event or is preceded by partial fluidization of the interface is a pertinent question. Once bed motion begins, the boundary condition becomes invalid and a new condition must be applied. A great deal of experimentation will be required to determine its form.

A direct extension of this paper is to determine the mean lift and drag forces on individual particles. Exact calculation of these forces is possible since the flow pattern at the interface is known. Fig. 14 shows a typical velocity profile and the lift and drag forces. The drag force F_D' contributes to the vertical force due to the moment about the contact point with the adjacent particle. The drag force is approximately equal to $\tau_0(\pi D^2/4)$, where D is the sediment particle diameter. The lift force F_L' is

$$\rho u_s\Gamma\approx\rho u_s\int\int(u_s)_z dA,$$

where Γ is the circulation about the particle and A represents area. The lift and drag forces are opposed by the submerged weight of the particle, i.e.,

$$F_g=-(\rho_s-\rho)g(\pi D^3/6).$$

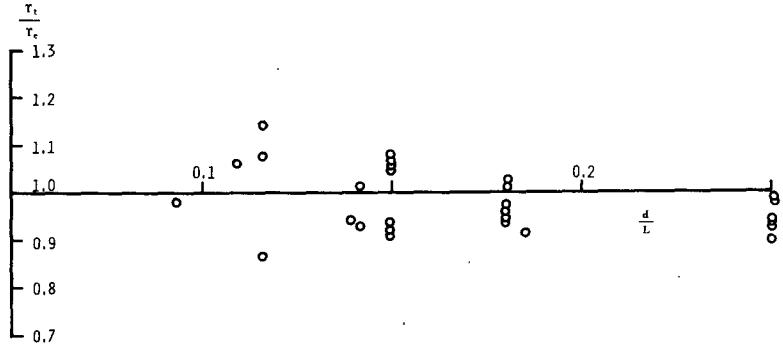

FIG. 13. Comparison of theoretical to experimental attenuation coefficients as a function of depth-to-wavelength ratio [data by Savage (1953)].

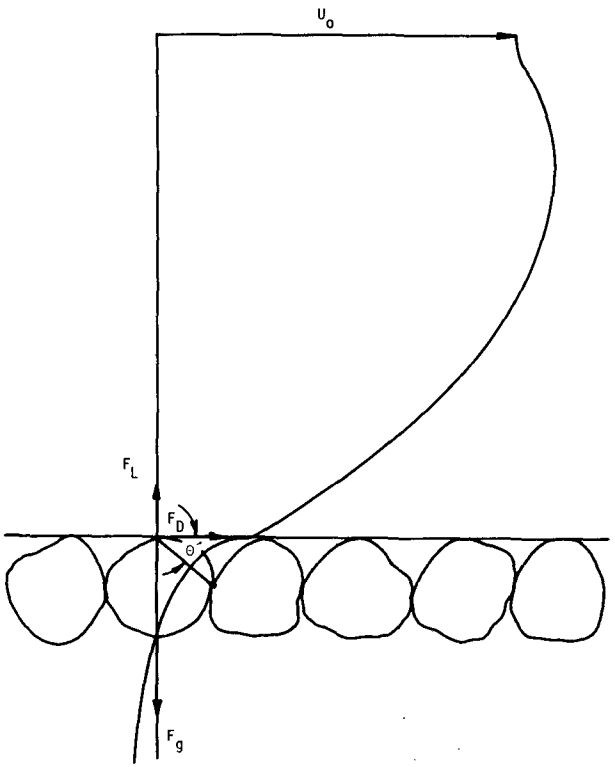

FIG. 14. Forces acting on a sediment particle.

With these calculations, the threshold conditions can be approximated analytically.

Acknowledgments. The authors would like to thank Drs. G. Janowitz and J. Machemehl of North Carolina State University for their assistance during the project of which this paper is a result. Also, the comments of the article's reviewers were greatly appreciated. The project was supported by the Center for Marine and Coastal Studies—NCSU, under Sea Grants PSR 139 and PSR 165 and North Carolina State University.

REFERENCES

Bagnold, R. A., 1963: Mechanics of marine sediments, Part 1. *The Sea*, Vol. 3, M. N. Hill, Ed., Interscience, 507–528.

Batchelor, G. K., 1974: Transport properties of 2-phase materials with random structure. *Annual Review of Fluid Mechanics*, Vol. 6, Annual Reviews, Inc., 227–255.

Beavers, G. S., and D. D. Joseph, 1967: Boundary conditions at a naturally permeable wall. *J. Fluid Mech.*, **30**, 197–207.

Brinkman, H. C., 1947: On the permeability of media consisting of closely packed porous particles. *Appl. Sci. Res.*, **A1**, 81–86.

Eckert, E. G., and R. M. Drake, Jr., 1959: *Heat and Mass Transfer*. McGraw-Hill, 530 pp.

Francis, J. R. D., 1973: Experiments on the motion of solitary grains along the bed of a water-stream. *Proc. Roy. Soc. London*, **A332**, 443–471.

Hough, S. S., 1896: On the influence of viscosity on waves and currents. *Proc. London Math. Soc.*, **28**, 264–288.

Hunt, J. N., 1959: On the damping of gravity waves propagated over a permeable surface. *J. Geophys. Res.*, **64**, 437–442.

Kajiura, K., 1968: A model of the bottom boundary layer in water waves. *Bull. Earthquake Res. Inst.*, **46**, 75–123.

Komar, P. D., and M. C. Miller, 1975: On the comparison between the threshold of sediment motion under waves and unidirectional currents with a discussion of the practical evaluation of the threshold. *J. Sediment. Petrol.*, **45**, 362–367.

——, R. H. Neudeck and L. D. Kulm, 1972: Observations and significance of deep-water oscillatory ripple marks on the Oregon continental shelf. *Shelf Sediment Transport*, Swift, Duane and Pilkey, Eds., Dowden Hutchinson and Ross, Chap. 25.

Liu, P., 1973: Damping of water waves over porous bed. *ASCE J. Hydrol. Div.*, **99**, **HY12**, 2263–2271.

Luikov, A. V., 1968: *Analytical Heat Diffusion Theory*. Academic Press, 685 pp.

Murray, J. D., 1965: Viscous damping of gravity waves over a permeable bed. *J. Geophys. Res.*, **70**, 2325–2331.

Phillips, O. M., 1969: *The Dynamics of the Upper Ocean*. Cambridge University Press, 261 pp.

Polubarinova-Kochina, P., 1962: *Theory of Ground Water Movement*. Princeton University Press, 613 pp.

Putnam, J. A., 1949: Loss of water wave energy due to percolation in a permeable sea bottom. *Trans. Amer. Geophys. Union*, **30**, 349–356.

Reid, R. O., and K. Kajiura, 1957: On the damping of gravity waves over a permeable sea bed. *Trans. Amer. Geophys. Union*, **38**, 662–666.

Richardson, S., 1971: A model for the boundary condition of a porous material. Part 2. *J. Fluid Mech.*, **49**, 327–336.

Rouse, H., 1961: *Fluid Mechanics for Hydraulic Engineers*. Dover, 442 pp.

Savage, R. P., 1953: Laboratory study of wave energy losses by bottom friction and percolation. Beach Erosion Board Tech. Memo. 31, 28 p.

Schlichting, H., 1968: *Boundary Layer Theory*. McGraw-Hill, 748 pp.

Taylor, G. I., 1971: A model for the boundary condition of a porous material. Part 1. *J. Fluid Mech.*, **49**, 219–326.

Teleki, P. G., and M. W. Anderson, 1970: Bottom boundary shear stresses on a model beach. *Proc. Conf. Coastal Engineering*, Part 1, Amer. Assoc. Civil Eng., 269–288.

Yang, C. T., 1973: Incipient motion and sediment transport. *ASCE J. Hydrol. Div.*, **99**, **HY10**, 1679–1704.